Dynamical Modeling of the Unsteady Flow over a Flapping Wing by applying Proper Orthogonal Decomposition and System Identification to Particle Image Velocimetry Data

Oguz Durmaz , H. Deniz Karaca, G. Deniz Ozen,
Cosku Kasnakoglu, D. Funda Kurtulus

Abstract— **In this work a novel approach for the dynamical modeling of the unsteady flow over a pitching airfoil is considered. The technique is based on collecting instantaneous velocity field data of the flow using particle image velocimetry (PIV), applying image processing to these snapshots to locate the airfoil, filling the airfoil and its surface with proper velocity data, applying proper orthogonal decomposition (POD) to these post-processed images to compute the POD modes and time coefficients, and finally fitting a discrete time state space dynamical model to the trajectories of the time coefficients using subspace system identification (N4SID). The procedure is implemented using MATLAB for the data obtained from a NACA0012 airfoil, and the results show that the dynamical model obtained can represent the flow dynamics with acceptable accuracy.**

I. INTRODUCTION

USING flapping wings to achieve flight is a topic of active research which has recently received significant attention in literature, especially in the area of Micro Aerial Vehicles (MAVs). Flapping wing MAVs have important advantages over conventional rotary-driven aircraft including higher maneuverability, increased efficiency, more lift, and reduced noise [1–3]. Understanding and modeling the aerodynamics of the flow of air over flapping wings is important since it can help improve these advantages. However, the aerodynamics of flapping motion is a complex nonlinear system because of the unsteady interaction between the vortex topologies and it is therefore difficult to model accurately. Efforts in this direction include the work by Kurtulus et. al. [4], Deng et. al. [5] and Zbikowski [6].

As it is the case for any flow process, physical meaning of the flow over flapping wings can be understood and analyzed mathematically by describing the flow in terms of velocity vectors and representing it with dynamical models. Navier-Stokes partial differential equations (PDEs) are the most commonly used set of equations that are capable of representing fluid flows very accurately; however, due to

their complexity they are very difficult to analyze and most of the time obtaining and analytical solution is not possible [7]. For this reason techniques such as Proper Orthogonal Decomposition (POD) are used to obtain a simpler representation of the velocity field and provide a convenient means to analyze the flow behavior. POD is a technique to decompose a flow velocity field into spatial modes (POD modes) and time-dependent amplitudes (time coefficients). The POD method extracts deterministic functions associated with large-scale energetic structures in a flow [8]. One can find many studies regarding fluid flows using POD methods including the work by on et. al. [9] on cylinder wakes , Rowley et. al. [7] regarding compressible isentropic flows and Bourguet et. al. [10] on transonic flows.

Since the POD technique requires instantaneous velocity information (i.e. snapshots) to decompose the flow, Particle Image Velocimetry (PIV) measurement technique can be used to obtain data for the unsteady velocity field. Examples of research using PIV include Scarano et. al. [11] who proposed an improved algorithm based on cross-correlation for the interrogation of PIV images and Daichin et. al. [12] who investigated the influence of a water surface on the structure of the trailing wake of a NACA0012 airfoil. It is also possible to use the PIV measurements as the set of snapshots required to obtain the POD modes [13-14]. Once the POD modes and time coefficients are obtained, techniques such as Galerkin Projection (GP) (Rowley et. al. [7], Gerhard et. al. [15]) or the System Identification (SI) (Khalil et. al. [16], Perret et al. [17]) can be used to derive a system of ODE's to represent the dynamics of these time coefficients.

In this paper we propose a systematic application of the techniques mentioned above (i.e. PIV, POD and SI) to the problem of obtaining dynamical models to represent the flow over a flapping wing (Section 2). The proposed approach is based on experimentally obtaining PIV snapshots of the flow, and then numerically processing these snapshots to construct the POD modes representing the flow process. The time coefficients representing the evolution of the flow over these modes are then obtained by projecting the snapshots over these modes. System identification techniques are then used to fit a dynamical model to these time coefficients. The flow is reconstructed using these dynamical models. The method proposed in the paper is applied to a flapping wing experimental setup (Section 3) and it is seen to be successful. The paper ends with conclusions and future works (Section 4).

II. METHODOLOGY

2-1) Instantaneous Flow Field Measurement using PIV Technique

Particle Image Velocimetry (PIV) is one of the non-intrusive measurement techniques that allows to observe the instantaneous flow field. [18]. It basically consists of a Nd:YAG laser, CCD camera, lens system. In the PIV system, different particles seed in the flow field are used to reflect the beam of Nd:YAG laser, which flashes in discrete time with a definite frequency to the CCD camera. Silver coated hollow sphere particles are used for the visualization of the vector field. The parameters for the PIV system used in this study are given in Table 1. The center of rotation is located at the quarter chord of the airfoil from the leading edge. The system of displacement is composed of two step motors. The first motor is allowing the translational motion and the second one, associated with the rotation of the wing. The useful rotational motion is of 360°. The pitching motion is carried out in zero free-stream velocity.

In order to extract the velocity information from the images of the particles, interrogation analysis is needed. PIV images are analyzed by dividing the images into small interrogation regions [19]. Smaller interrogation window size is preferable because it can give better spatial resolution of the PIV measurements. However, if the windows size is too small, it can cause inaccurate velocity vectors. Interrogation is done by adaptive cross correlation method [20-21]. In our setup this process is carried out by Dynamic Studio program [22]. A schematic illustration of the PIV setup used in our experiments is shown in Figure 1.

Before the POD method can be applied, instantaneous velocity field data of the flow must be obtained, which is done in this work by using a PIV setup. In this paper the results for the symmetrical NACA0012 airfoil will be presented. The pitching motion of the airfoil is provided by a motor, which is mounted on the traverse system. The period of the pitching motion is 10 s and maximum angular velocity is 0.63 rad/s. The motor is connected to the quarter chord of the airfoil; therefore angular displacement of quarter chord is zero. The signals that provide the movement of the motors are generated by a MATLAB/Simulink program. The camera and Nd:YAG laser operate in synchronized fashion to capture the reflection from the particles. The captured double images are processed by Dantec Studio program employing adaptive cross correlation method. This is used to construct the velocity vectors by finding differences between sequential snapshots [23]. The output of the program is the velocity vector fields, i.e. the x and y velocities of the snapshots, which then imported into MATLAB. To use the PIV data for POD and SI, a preprocessing of the snapshots is needed in order to determine the geometry of the airfoil; this must be done at each time instant since the airfoil is in motion (Figure 2). For this purpose an image processing algorithm in MATLAB was developed for masking the airfoil. By using MATLAB Image Processing Toolbox, techniques like image enhancement, noise elimination, morphological operations and edge detection was applied in proper sequence to each PIV snapshot, to determine the geometric properties of the airfoil such as the leading edge, trailing edge, quarter chord location, coordinates of its surface and angle of attack.

Once the geometry of the airfoil is obtained by the image processing algorithm described above, velocity information is added inside the airfoil and its surface. This is necessary because in the flow field the streamlines cannot penetrate the airfoil since it is a solid body. In addition, the POD method requires that the velocity information be available for all points of the snapshots. The airfoil performs a sinusoidal pitching motion, where the instantaneous angle of attack α in radians is given by

$$\alpha(t) = \alpha_0 sin\,(2\pi f t) \qquad (1)$$

where $\alpha_0 = \pi/6$, $f = 0.1\,Hz$ is the frequency of the motion, and t is the time variable. The angular velocity ω in rad/s with respect to the quarter chord of the airfoil is given by the expression

$$\omega(t) = \frac{d\alpha(t)}{dt} = 2\pi f \frac{\pi}{6} cos(2\pi f t) \qquad (2)$$

Since the x-y coordinates of the airfoil's surface and the angular velocity ω is known for each snapshot, the velocity vectors $\boldsymbol{U}(x,y)$ inside the moving airfoil and on its surface can be calculated by

$$\boldsymbol{U}(x,y) = \boldsymbol{r}(x,y) \times \omega \boldsymbol{k} \qquad (3)$$

where $\boldsymbol{r}$ is the position vector relative to the quarter chord and $\boldsymbol{k}$ is the unit vector in the z-direction.

2-2) Applying POD to the Snapshots to Obtain the POD Modes and Time Coefficients

Proper Orthogonal Decomposition is an effective method of data analysis using which high-dimensional processes can be described by low-dimensional approximations. A flow velocity field can be decomposed into spatial modes and time-dependent amplitudes by using POD. This method is also known as *the Karhunen-Loeve Decomposition* and *the single value decomposition* [8]. In order to apply POD, snapshots are collected from an experimental or a numerical system. For our case, unsteady velocity measurements around four different airfoils, namely, NACA0012, SD7003, elliptical and flat plate are collected by using PIV technique. After collecting the data, POD technique produces a set of basis functions which optimally represents the spatial distribution of the snapshots collected. Each POD basis function captures a certain percentage of the energy of the flow field [19,24]. One can choose a certain number (N) of POD modes to capture a sufficient amount of the flow energy and then represent the flow field as a finite dimensional approximation as

$$U(x, y, t) \approx \sum_{i=1}^{N} a_i(t) \phi_i(x, y) \qquad (4)$$

where a_i, $i = 1,2, \dots, N$ are called *time coefficients* and ϕ_i represents the *POD modes* of the ensemble.

To obtain the POD modes ϕ_i of the flow field, one first obtains a set of instantaneous velocities (snapshots) U_i where $U_i(x, y) = U(x, y, t_i)$ and t_i is the ith time instant where measurements are taken. The average of the ensemble of snapshots can then be defined as

$$\bar{U}(x, y) = \langle U \rangle = \frac{1}{M} \sum_{i=1}^{M} U_i(x, y) \qquad (5)$$

where M is the number of snapshots. Then, a new set of snapshots (V_i) are obtained by subtracting this mean value from each velocity measurement
$V_i(x, y) = V(x, y, t_i)$
$$= U(x, y, t_i) - \bar{U}(x, y) = U_i(x, y) \qquad (6)$$
$$- \bar{U}(x, y)$$

Then the $M \times M$ spatial correlation matrix C of the ensemble is constructed as follows

$$C_{ij} = \frac{1}{M} \int \int V_i(x, y) V_j(x, y) dx \, dy, \qquad (7)$$
$$i = 1, \dots, M, \qquad j = 1, \dots, M$$

The POD modes ϕ_i of the flow field can then be obtained by solving the eigenvalue equation;

$$C \phi_i = \lambda_i \phi_i \qquad (8)$$

That is, the POD modes ϕ_i are the eigenvectors of the correlation matrix C. The eigenvalue λ_i represent the amount of energy of the flow field captured by the ith POD mode ϕ_i. Based on this energy information, one can decide on the number of POD modes (N) to include in the approximation (4). It can be shown that the POD modes obtained using this procedure is orthonormal, i.e. they satisfy

$$\frac{1}{M} \int \int \phi_i(x, y) \phi_j(x, y) dx \, dy = \begin{cases} 1, & if \ i = j \\ 0, & if \ i \neq j \end{cases} \qquad (9)$$

Once the POD modes are obtained, the time coefficients a_i of the flow field can be obtained by projecting the snapshots onto the POD modes

$$a_i(t_j) = \frac{1}{M} \int \int V(x, y, t_j) \phi_i(x, y) dx \, dy, \qquad (10)$$
$$i = 1, \dots, N, \qquad j = 1, \dots, M$$

The details of the POD procedure can be found in Holmes et al. [25] and Sirovich [26].

Proper Orthogonal Decomposition (POD) method is applied to the post-processed PIV snapshots of the pitching airfoil in order to obtain an expansion of the form given in (4). For this purpose PIV data for 5 periods of the pitching motion is used, which consists of 250 snapshots. POD modes of unsteady velocity measurements are found as

described above. Then, time coefficients are calculated by taking projection of snapshots on the POD modes as in (10).

2-3) System Identification

Once the POD modes are obtained and the flow is expanded as in (4), it can be observed that the time variation is dictated only by the coefficients a_i because the modes Φ_i depend only on the spatial variables and not the time variable. Hence to model the flow dynamics it is sufficient to fit a suitable dynamical model to the trajectories of the time coefficients $a_i(t)$. For this purpose we will derive a state-space model of the following form:

$$\xi(t + T_s) = A\xi(t) + B\gamma(t) \qquad (11)$$

$$y(t) = C\xi(t) + D\gamma(t) \qquad (12)$$

where $\xi \in \mathbb{R}^n$ is the state vector, $n \in \mathbb{N}$ is the degree of the system, $\gamma \in \mathbb{R}$ is control input and $\gamma \in \mathbb{R}^n$ is the output signal. Since the flow snapshots are obtained at discrete time intervals separated by a sampling period of $T_s \in \mathbb{R}$ seconds, the model above is a discrete-time state space model. The matrices A, B, C and D determine the dynamical system and are to be obtained by constructing a model from (11) and (12) using system identification techniques. For this purpose input-output data must be collected for the system which is usually done by applying various input signals (e.g. sine waves, ramp functions and chirp signals) and recording the resulting outputs, which are the time coefficients of the expansion, i.e.

$$y(t) = a(t) = [a_1(t) \, a_2(t) \dots a_N(t)]^T \qquad (13)$$

where N is the number of POD modes used in the expansion. From the input-output data, subspace system identification method (N4SID) is used for obtaining the A, B, C and D matrices in (11) and (12). The main idea behind the subspace method is to first estimate the extended observability matrix:

$$Q_r = \begin{bmatrix} C \\ CA \\ \vdots \\ CA^{r-1} \end{bmatrix} \qquad (14)$$

for the system from input–output data by direct least-squares-like projection steps. In particular, it is possible to show that an expression of the form

$$Y_r(t_k) = Q_r \, \xi(t_k) + S_r \Gamma_r(t_k) + V(t) \qquad (15)$$

can be obtained from (11) and (12), where

$$Y_r(t_k) = \begin{bmatrix} Y(t_k) \\ Y(t_{k+1}) \\ \vdots \\ Y(t_{k+r-1}) \end{bmatrix} \qquad (16)$$

$$\Gamma_r(t_k) = \begin{bmatrix} \gamma(t_k) \\ \gamma(t_{k+1}) \\ \vdots \\ \gamma(t_{k+r-1}) \end{bmatrix} \tag{17}$$

$$S_r = \begin{bmatrix} D & 0 & \cdots & 0 & 0 \\ CB & D & \cdots & 0 & 0 \\ \vdots & \vdots & \ddots & \vdots & \vdots \\ CA^{r-2}B & CA^{r-3}B & \cdots & CB & D \end{bmatrix} \tag{18}$$

and $V(t)$ is the contribution because of output noise. The extended observability matrix Q_r can then be estimated from (15) by correlating both sides of the equality with quantities that eliminate the term $S_r\Gamma(t_k)$ and make the noise influence from $V(t)$ disappear asymptotically. Once Q_r is known, it is possible to determine C and A by using the first block row of Q_r and the shift property, respectively. Once A and C are at hand, B and D are estimated using linear least squares on the following expression

$$y(t_k) = C(zI - A)^{-1}B\gamma(t_k) + D\gamma(t_k) \tag{19}$$

where Equation (19) is a representation of the system described by (11) and (12) in terms of the time-shift operator z. Details of the subspace method for estimating state-space models can be found in Ljung [27], Van Overschee [28] and Larimore [29].

In this work, MATLAB System Identification Toolbox is used to construct a dynamical system for the time coefficients, which were obtained in the previous step by projecting the snapshots on the POD modes as in (10).

III. RESULTS

In this section, the results of applying the methodology described in the previous section to obtain a dynamical model for the pitching motion of the NACA0012 airfoil is presented. The first task is to conduct experiments and collect velocity data using the PIV setup as described in Section 2. A few of the images obtained from the PIV measurements are shown in Figure 2. One can see the laser illuminated seeding particles, which appear white in the figure, and the airfoil in motion, which appears black. Then, velocity vectors are obtained from the PIV images for 5 periods using Dantec Dynamic Studio. Next, the instantaneous location of the airfoil is determined using the image processing techniques described in Section 2. Figure 3 shows the instantaneous velocity field in the x directions with the appropriate airfoil location superimposed on the image. Prior to applying POD to these snapshots, the velocity information inside the airfoil and its surface is filled in using expression (3) and the mean value of the flow is removed. The x component of the first nine POD modes resulting from applying POD to the flow snapshots is shown. The first mode is the highest energy mode and captures the dominant characteristics of the flow. The subsequent modes reveal additional details of the flow behavior. The number of POD modes to include in the expansion (4) is selected based on how much of the flow energy (and thus the amount of detail) one wishes to include

in the approximation. Including a high number of modes will yield a better approximation but will increase the complexity of the resulting model. In this work, we have chosen to include 100 modes out of 250, which corresponds roughly to 98.93% of the flow energy (see Figure 5). To verify that the selected number of modes can represent the flow accurately, we obtain a reconstruction of the flow using (4), where the time coefficients a_i are obtained by projecting the flow snapshots onto the POD modes as expressed in (10). The x components of the reconstructed flow velocity is shown in Figure 6. It can be observed that the reconstructed flow velocity is quite similar to snapshots obtained from PIV shown in Figure 3. The next step is to fit a dynamical model to the time coefficient data using N4SID system identification technique. This procedure is carried out using MATLAB system identification and a discrete time state space dynamical model of the form (11)-(12) is obtained. The order of this model turned out to be 40. To evaluate how well this model approximates the POD time coefficients, we first run this model for the length of five periods (50 seconds) and compare the output of the model with the POD time coefficients. This comparison is presented in Figure 7. It can be seen that the model output is acceptably close to the POD time coefficients. Hence, it can be stated that the dynamical model is successful in capturing the time variation of the flow. As a final test, we perform a reconstruction of the flow using the dynamical model's output as a_i's in (4), the results of which is shown in Figure 8. Comparing this figure with the original PIV snapshots in Figure 3, one can see that the results are sufficiently close to each other. Therefore the model obtained using the procedure described in the paper can represent the flow with acceptable accuracy and can be used for various analysis and design tasks.

IV. CONCLUSIONS AND FUTURE WORKS

In this paper a modeling approach to represent the dynamical behavior of a pitching airfoil is considered. It was seen that the model represents the flow with acceptable accuracy. Such a mathematical model can be used in analyzing certain characteristics of the flow (e.g. stability) or performing certain synthesis tasks (e.g. controller design). Future research directions include applying the devised method to different airfoil data that were also collected in our PIV experiments, namely data for SD7003, elliptical and flat plate.

V. REFERENCES

[1] A. Azuma, O. Masato, Y. Kunio, Aerodynamic characteristics of wings at low Reynolds Numbers. Fixed and flapping wings aerodynamics for micro air vehicle applications, In Progress in Astro. & Aero., vol. 195, Mueller TJ , (2001) 341–398.

[2] R. S. Fearing, K. H. Chiang, M. H. Dichinson, Wing transmission for a micromechanical flying insect, Proceedings of the 2000 IEEE, International Conference on Robotics & Automation, San Francisco, CA, (2000) 1509–1516.

[3] S. Ho, H. Nassef, N. Pornsinsirirak, Unsteady aerodynamics and flow control for flapping wing flyers, Progress in Aerospace Science (2003) 635–681.

[4] X. Deng, L. Schenato, S. S. Sastry, Model identification and attitude control scheme for a micromechanical flying insect, International Conference on Robotics and Automation, Taiwan (2003).

[5] D. F. Kurtulus, L. David, A. Farcy, N. Alemdaroglu, Aerodynamic characteristics of flapping motion in hover, Exp fluids (2008) 44: 23-36.

[6] R. Zbikowski, On aerodynamic modeling of an insect-like flapping wing in hover for micro air vehicle, Phil. Trans. R. Soc. Lond A (2002) 273-290

[7] C. W. Rowley, T. Colonius, R. M. Murray, Model reduction for compressible flows using POD and Galerkin projection. Physica D 189 (2004) 115-129.

[8] T. N. Erbil, C. Kasnakoglu, Feedback flow control employing local dynamical modeling with wavelets, Mathematical and Computer Modeling of Dynamical Systems, iFirst (2009) 1-21.

[9] B. R. Noack, K. A. Siev, M. Morzyinski, G. Tamor, F. Thiele, A hierarchy of low-dimensional models for the transient and post-transient cylinder wake, Journal of Fluid Mechanics. (2003) 497: 335-363.

[10] R. Bourguet, M. Braza, A. Dervieux, Reduced-order modeling for unsteady transonic flows around an airfoil, Phys. Fluids. 19:111701 (2007) 1-4.

[11] F. Scarano, M. L. Riethmuller, Iterative multigrid approach in PIV image processing with discrete window offset, Experiments in Fluids 26 (1999) 513-523.

[12] Daichin, W. Kang, L. Zhao, PIV Measurements of the near wake flow of an airfoil above a free surface, Science Direct Journal of Hydrodynamics Ser.B 19(4) (2007) 482-487.

[13] P. Druault, C. Challiou, Use of proper orthogonal decomposition for reconstructing the 3D in-cylinder mean-flow Field from PIV data, Comptes Rendus Mécanique, Vol. 335, No. 1 (2007) 42-47.

[14] P. Guibert, F. Alizon, P. Druault, Use of proper orthogonal decomposition for time interpolation from PIV data, Experiments in Fluids, Vol. 39 No. 6 (2005) 1009-1023.

[15] J. Gerhard, M. Pastoor, R. King, B. R. Noack, A. Dillmann, M. Morzynski, G. Tadmor, Model-based control of vortex shedding using low-dimensional Galerkin models, AIAA Paper. (2003)

[16] M. Khalil, S. Adhikari, A. Sarkar, Linear system identification using proper orthogonal decomposition, Mechanical Systems and Signal Processing, Vol. 21, No. 8 (2007) 3123-3145.

[17] L. Perret, J. Delville, E. Collin, Polynomial identification of POD based low-order dynamical system, Journal of Turbulence, Vol. 7, No. 17 (2006)

[18] M. Raffel, C. Willert, S. Wereley, J. Kompenhans, Particle image velocimetry: a practical guide, Springer Science & Business, New York, 1998.

[19] D. M. Lucthenburg , B. R. Noack, M. Schlegel, An introduction to the POD and Galerkin method for fluid flows with analytical examples and MATLAB source codes, Berlin Institute of Technology, Technical Report (2009).

[20] J. Kostas, J. Soria, M. Chong, Particle image velocimetry measurements of a backward- facing step flow, Experiments in Fluids 33 (2002) 838-853.

[21] O. Uzol, J. Katz, Flow measurement techniques in turbomachinery, in: Springer Handbook of Experimental Fluid Mechanics, Section 14 (2007) 919-958.

[22] Particle Image Velocimetry measurement principles, Dantec Dynamics, http://www.dantecdynamics.com/Default.aspx?ID=1049 (2010).

[23] B. Galletti, A. Bottaro, C. H. Bruneau, A. Iollo, Accurate model reduction of transient and forced wakes, European Journal of Mechanics - B/ Fluids 26 (2007) 354–366.

[24] A. Chatterjee, An introduction to the proper orthogonal decomposition, Current Science, vol. 78, no. 7 (2000) 808-817.

[25] P. Holmes, J. L. Lumley, G. Berkooz, Turbulence, coherent structures, dynamical system, and symmetry, Cambridge University Press, 1996.

[26] L. Sirovich, Turbulence and the dynamics of coherent structures, Quarterly of Applied Mathematics, 45 (1987) 561-590.

[27] L. Ljung, System Identification: Theory for the User, PTR Prentice Hall, Upper Saddle River, NJ, 1999.

[28] P. Van Overschee, B. De Moor, Subspace identification for linear systems: Theory-Implementation-Applications, Kluwer Academic Publishers, Dordrecht, 1996.

[29] W. E. Larimore, Statistical optimality and canonical variate analysis system identification, Signal Process. 52 (1996) 131–144.

TABLE 1: FLOW PROPERTIES AND PIV PARAMETERS

|		
Airfoil	Type	NACA0012
	Chord	c = 0.06 m
Flow	Fluid	Water
	Temperature [°C]	21
Motion	Period [s]	10
	Max. Angular Velocity [rad/s]	0.63
Seeding	Type	Silver Coated Hollow Glass Spheres
	Diameter [µm]	10
	Concentration [g/cm^3]	0.0000475
Laser	Type	Nd:YAG
Recording	Camera Type	CCD FlowSense 2M/E
	Number of Camera	1
	Lens Focal Length [mm]	60
	Frame Rate [Hz]	5
	$\Delta t/T$	0.02
	Resolution [pixels]	1600 x 1200
	Exposure Delay Time [µs]	10000
Interrogation	Method	Double Frame & Adaptive Cross Correlation
	Resolution	32 x 32 pixels with 50% overlap
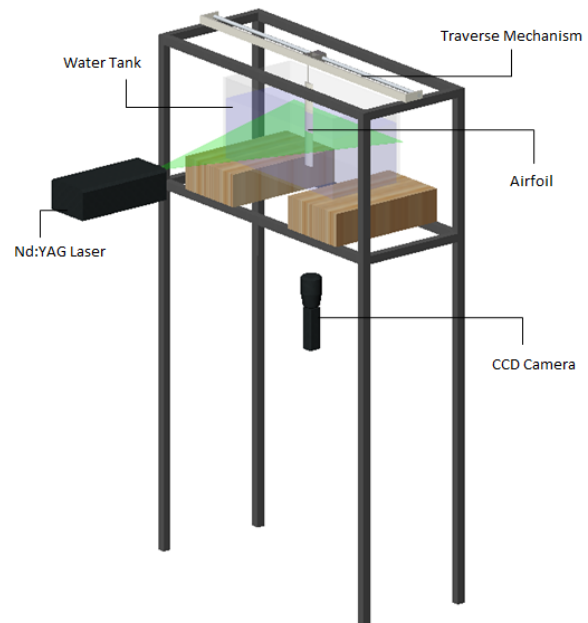
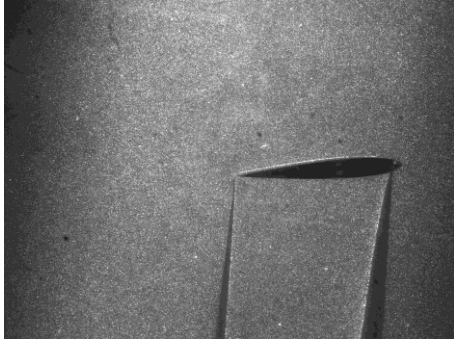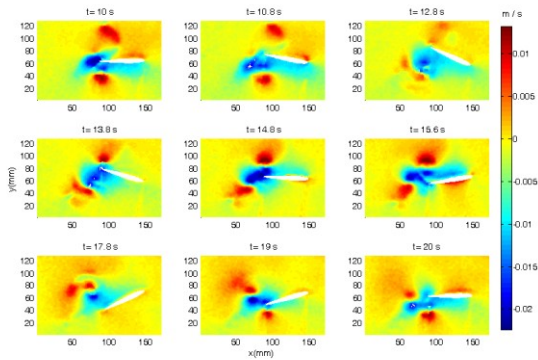Figure 1: Schematic illustration of PIV setup

Figure 2: Instantaneous PIV Images of pitching NACA0012 airfoil

Figure 3: X Velocity Components of the PIV Snapshots during the second period
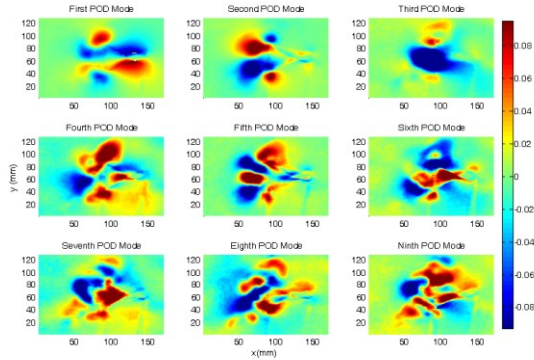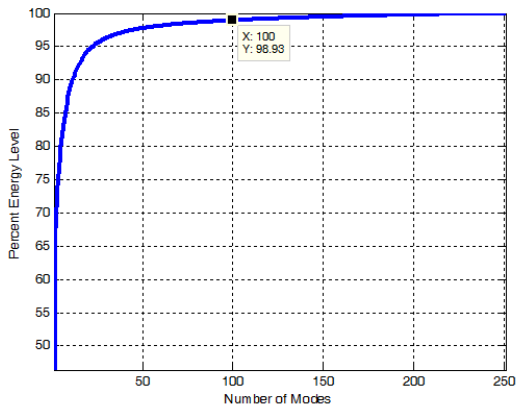

Figure 4: POD Modes in X Direction

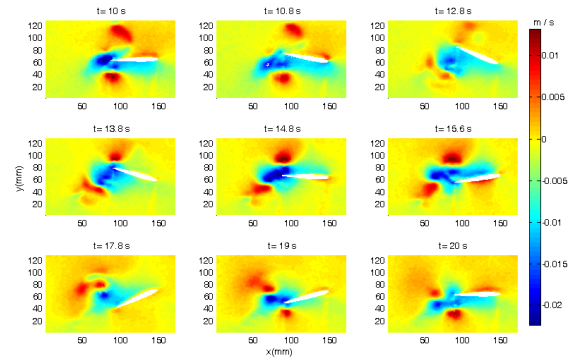Figure 5: Energy Level vs Number of POD Modes

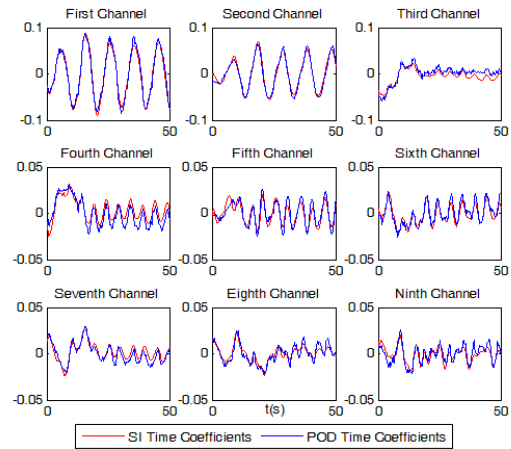Figure 6: X Velocities Reconstructed with POD Time Coefficients
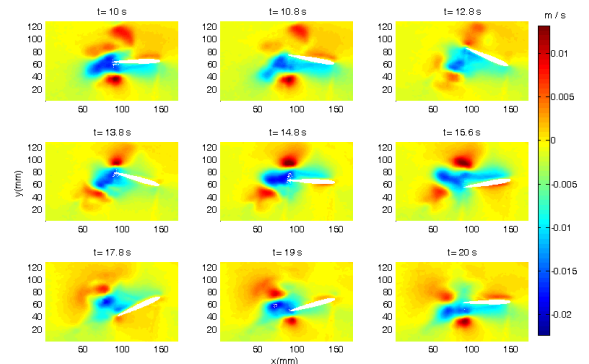

Figure 7: Channel Output

Figure 8: X Velocities Reconstructed with System Identification Time Coefficients